

# DAMAGE AND FAILURE MECHANISMS ASSOCIATED WITH PHOTOABLATION OF BIOLOGICAL TISSUES

Tarabay Antoun, Lynn Seaman, Donald Curran

*Poulter Laboratory, SRI International, 333 Ravenswood Avenue, Menlo Park, CA 94025*

Michael Glinsky

*Lawrence Livermore National Laboratory, 7000 East Avenue, P.O. Box 808, Livermore, CA 94551*

This paper aims to examine the processes associated with failure of the cornea and other collagenous tissues during photoablation. Two different constitutive models are applied to simulate a series of laser deposition experiments into porcine reticular dermis (1), a biological tissue similar to the cornea in composition and photoablation characteristics. The first of our constitutive models, DFRACT, is a physically motivated, micromechanical model based on the nucleation and growth of spherical voids (2). The second is a relatively simple model that allows the material to vaporize and thermally soften. The simulation results reproduce the prominent features observed experimentally thereby shedding a new light on the operative mechanisms during photoablation. The good qualitative agreement between the simulated stress histories and the stress histories measured during the experiments also demonstrates the effectiveness of micromechanical damage and failure modeling as a viable tool for optimizing existing laser surgery procedures and designing new ones.

## INTRODUCTION

Despite the widespread use of lasers in medical applications, the physical phenomena associated with laser-tissue interactions are still not very well understood. This is partially due to the complex structure of biological tissue and to the influence this structure has on the absorption characteristics of the tissue. In this paper, we attempt to shed new light on the damage and failure mechanisms associated with photoablation of biological tissues. This is accomplished by simulating the response of porcine reticular dermis to the deposition of laser energy and comparing the simulation results with the experimental data of Venugopalan (1).

## EXPERIMENTAL STUDY

The experimental configuration of the laser deposition experiments performed by Venugopalan on biological tissue is shown schematically in Fig. 1. This configuration consisted of a porcine dermis layer approximately 400- $\mu\text{m}$ -thick, and a thick, impedance-matched layer of saline solution. A thin

PVDF film sandwiched between the two layers was used to record the stress history at the back surface of the tissue sample. The laser beam diameter was 1 mm or larger, thus ensuring 1-D strain conditions throughout the experiment.

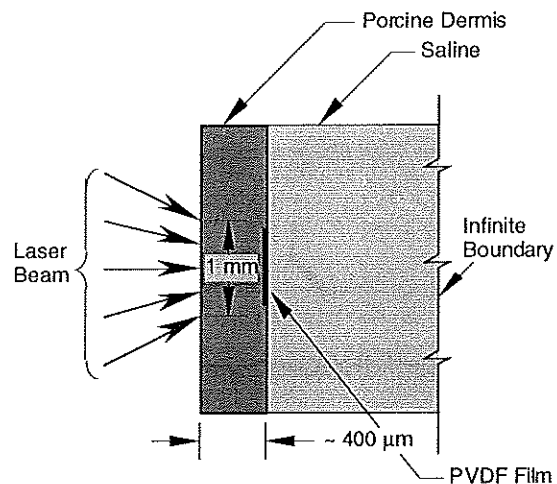


FIGURE 1. Experimental configuration of the laser deposition experiments.

Porcine dermis, as well as other collagenous tissues, is composed of two primary energy-absorbing components: water, which accounts for about 70% of the total mass, and collagen fibers, which form the reticular extracellular matrix (ECM) and account for the majority of the remaining 30% of the total mass. Two lasers, carefully chosen to selectively target either the water or the ECM of the tissue, were used in the experiments simulated in the present study. The first is a 248-nm Kr-F excimer laser which selectively targets the extracellular matrix of the tissue. This laser has an absorption depth of 30  $\mu\text{m}$  and a pulse duration of 24 ns. The second is a 10.6- $\mu\text{m}$  TEA CO<sub>2</sub> laser which targets the tissue water. It has an absorption depth of 20  $\mu\text{m}$  and a pulse duration of 30 ns.

Stress histories at several different levels of radiant exposure are shown in Fig. 2 and Fig. 3 for tissue samples irradiated with the Kr-F excimer laser and the TEA CO<sub>2</sub> laser, respectively. With increasing fluence, both figures appear to indicate a gradual loss of strength as evident by the progressive deterioration of the ability of the material to propagate the tensile component of the

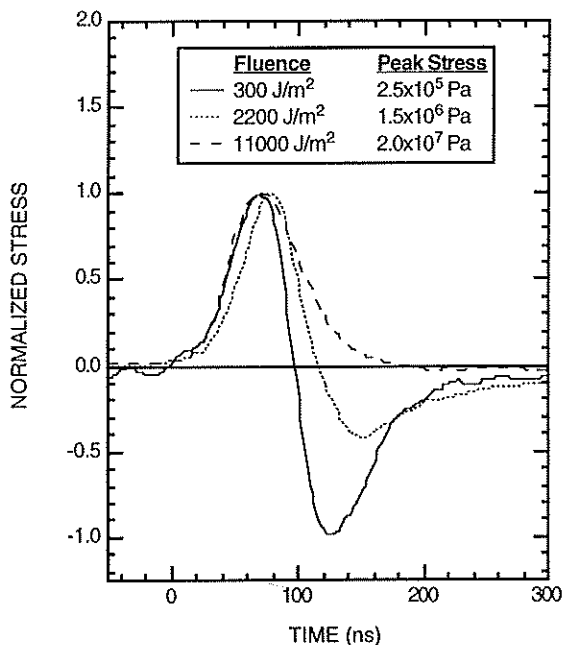


FIGURE 2. Stress histories recorded with a PVDF transducer 400  $\mu\text{m}$  away from the surface of porcine dermis samples irradiated using a 248-nm Kr-F excimer laser (1).

bipolar stress pulse. This is an indication that failure has occurred in the interior of the sample. The transitions from fully elastic behavior to inelastic behavior then failure in Fig. 2 and Fig. 3 proceed in two different manners as evidenced by the different characteristics of the intermediate stress pulses in the two figures. In the remainder of this paper, we describe two constitutive models and associated simulation results that will help explain the trends in the experimental data in terms of underlying damage and failure mechanisms.

### CONSTITUTIVE MODELS

Two constitutive models were used to represent porcine dermis in our hydrocode simulations. For the case where the extracellular matrix (ECM) is the primary chromophore of the laser radiation, we modeled the material using DFRACT - a physically motivated, micromechanical model based on the nucleation and growth of spherical voids and the manner in which they affect the strength and subsequent deformation of the material (2). The damage evolution, in terms of the number of voids

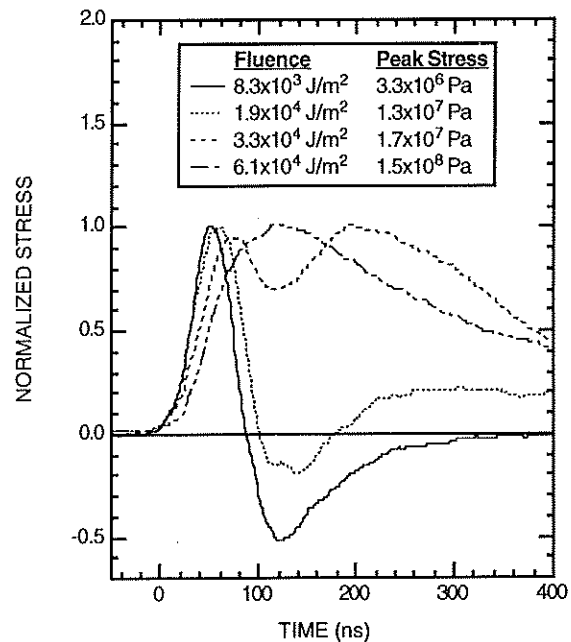


FIGURE 3. Stress histories recorded with a PVDF transducer 400  $\mu\text{m}$  away from the surface of porcine dermis samples irradiated using a 10.6- $\mu\text{m}$  TEA CO<sub>2</sub> laser (1).

per unit volume and the void size, is monitored in the model with two rate equations that depend on the yield strength, the number of nucleation sites, the initial flaw size, and the viscosity of the material. These model parameters were chosen to be representative of the properties of collagen fibers.

For the case where tissue water is the primary chromophore of the laser energy, the material was represented by a simple model that allows the biological tissue to vaporize and thermally soften. In the model, vaporization occurs when the internal energy exceeds the sublimation energy, the value of which was chosen to reproduce the trends in the data. The thermal softening model simply reduces the yield strength of the tissue from its initial value at room temperature to zero when the internal energy becomes equal to the melt energy (assumed to be equal to the sublimation energy).

The pressure-volume response of the tissue was modeled using the equation of state of water, and the energy deposition profile was described using the Beer-Lambert equation. The simulations were performed using the one-dimensional finite difference hydrocode SRI PUFF (3).

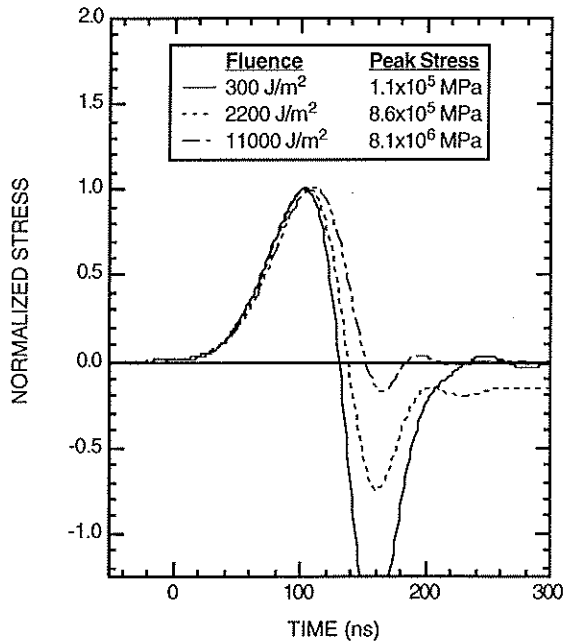


FIGURE 4. Simulated stress histories 400  $\mu\text{m}$  away from the surface of porcine dermis samples irradiated using a 248-nm Kr-F excimer laser. Results obtained by allowing the material to fail by void nucleation and growth under tension.

## HYDROCODE SIMULATION RESULTS

The stress histories simulated using the DFRAC model and the thermal softening and vaporization model are shown in Fig. 4 and Fig. 5, respectively. The radiant exposures (i.e., fluences) used in the simulations are the same as those used in the experimental studies the results of which are shown in Fig. 2 and Fig. 3. A comparison of the simulation results in Fig. 4 with the experimental data in Fig. 2 shows a good qualitative agreement, as does a similar comparison of Fig. 5 and Fig. 3.

In Fig. 4, the transition from elastic behavior at a fluence of 300 J/m<sup>2</sup>, to complete fracture at a fluence of 11000 J/m<sup>2</sup> is due to nucleation and growth of spherical voids. This is further illustrated in Fig. 6 where the void volume fraction at the end of the simulation for each of the three fluence levels is plotted (on a logarithmic scale) as a function of Lagrangian distance. As can be seen in this figure, the void volume fraction associated with the lowest fluence is on the order of 10<sup>-8</sup> indicating an essentially elastic behavior. On the other hand, the void volume fraction associated with the highest fluence level is approximately 0.25

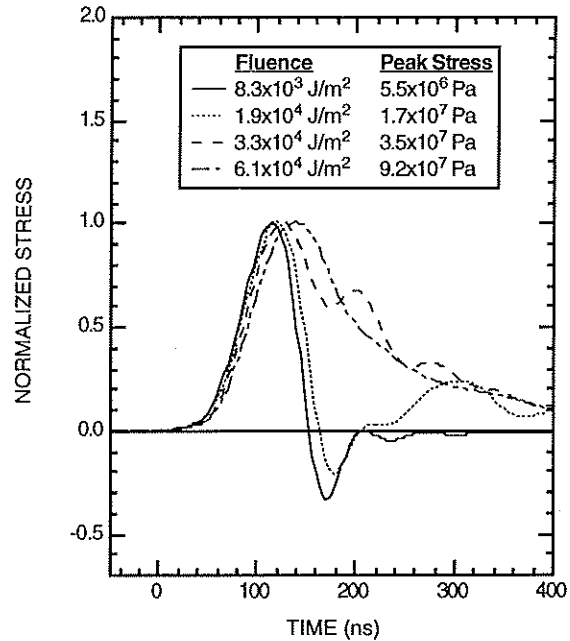


FIGURE 5. Simulated stress histories 400  $\mu\text{m}$  away from the surface of porcine dermis samples irradiated using a 10.6- $\mu\text{m}$  TEA CO<sub>2</sub> laser. Results obtained by allowing the material to vaporize and/or thermally soften.

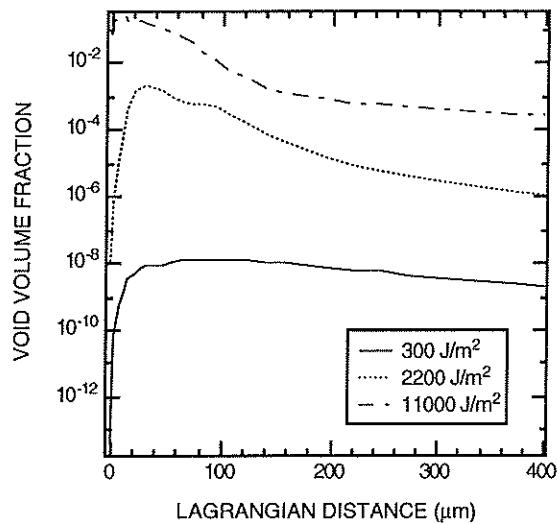


FIGURE 6. Simulated void volume fraction as a function of distance for the porcine dermis samples irradiated using a 248-nm Kr-F excimer laser.

indicating that voids occupy about 25% of the volume. At this fluence level, Fig. 4 shows that the ability of the material to support tensile loads is nearly diminished.

Fig. 7 shows snapshots of damage distribution across the first half of the specimen. As shown, damage is concentrated in a region about 100  $\mu\text{m}$  wide near the front surface. The material at and near the gage section remains elastic throughout the simulation.

The wave structures observed in Fig. 5 can be explained in terms of thermal softening and front surface vaporization. At the lowest fluence, the tissue does not vaporize, but the energy level is close enough to the melt energy that the material near the front surface thermally softens causing a reduction in the peak tensile stress magnitude. As the fluence increases, a layer of tissue vaporizes near the front surface of the specimen. The usually-bipolar thermoelastic stress pulse is perturbed by two additional stress disturbances: one originating at the vapor-liquid boundary and the other at the boundary between the layer of material within the laser deposition depth and the rest of the specimen. The latter of these disturbances dominates the response at a fluence of  $1.9 \times 10^4 \text{ J/m}^2$  and the former dominates the response at a fluence of  $3.3 \times 10^4 \text{ J/m}^2$  leading to the "double-pulse" structure in the wave profile.

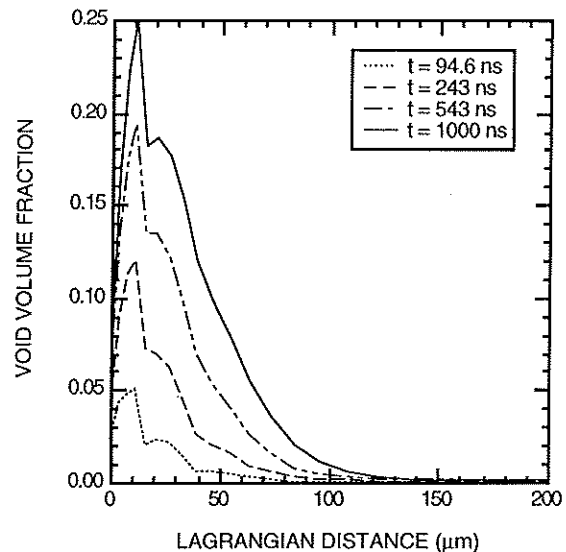


FIGURE 7. Simulated damage (void volume fraction) evolution in the porcine dermis sample irradiated using a 248-nm Kr-F excimer laser at a fluence of  $1.1 \times 10^4 \text{ J/m}^2$ .

As the fluence is increased to  $6.1 \times 10^4 \text{ J/m}^2$ , the whole layer of material within the deposition depth vaporizes. As such, the two disturbances associated with the intermediate fluence levels merge into a single disturbance leading to the "single-pulse" structure in the wave profile depicted in Fig. 5.

## CONCLUSION

The study described here demonstrates that micromechanical damage modeling combined with hydrocode simulations is a useful and effective tool that can be used to interpret experimental data, optimize existing laser surgery procedures, and provide guidance for designing new procedures.

## REFERENCES

1. Venugopalan, V., "The Thermodynamic Response of Polymers and Biological Tissues to Pulsed Laser Irradiation," PhD Dissertation, Massachusetts Institute of Technology, May 1994.
2. Seaman, L., Curran, D. R., Aidun, J. B., and T. Cooper, "A Microstatistical Model for Ductile Fracture with Rate Effects," *Nuclear Eng. and Design* 105, 35-42 (1987).
3. Seaman, L. and Curran, D. R., "SRI PUFF 8 Computer Program for One-Dimensional Stress Wave Propagation," SRI International Final Report (vol. II) prepared for the Army Ballistics Research Laboratory, August, 1978.